RSC Advances

An *ab initio* study on the electronic and magnetic properties of MgO with intrinsic defects

Fang-Guang Kuang[1], *Shu-Ying Kang*[1], *Xiao-Yu Kuang*[1a)], and *Qi-Feng Chen*[2]

[1]Institute of Atomic and Molecular Physics, Sichuan University - Chengdu 610065, China

[2]Laboratory for Shock Wave and Detonation Physics Research, Institute of Fluid Physics, Chinese Academy of Engineering Physics, Mianyang 621900, China

Using *ab initio* calculations based on density functional theory with PBEsol/PBEsol+U method, the electronic and magnetic properties of undoped MgO are investigated. Calculated results demonstrate that both neutral (V_{Mg}^0) and singly charged Mg vacancy (V_{Mg}^-) can introduce magnetic moment to MgO, and the magnetic moment mainly arises from the spin polarization of the partially occupied 2p orbitals of nearest O atoms. In combination of group theory and molecular orbital theory, it is found that the magnetic moment is origin from the partially occupied e_g- orbital. Results also demonstrate that closed shell Mg vacancy (V_{Mg}^{2-}) and all of V_O^0, V_O^+ and V_O^{2+} can not lead to magnetic moment in MgO, but V_O^+ and V_O^{2+} will change the insulating behavior into n-type conductivity. In MgO with double Mg vacancies, the defects formation energies suggest that two Mg vacancies prefer the next nearest sites to other configurations. And the magnetic coupling induced by two Mg vacancies is mainly due to the p-p hybridization interaction of O atoms. However, the magnetic moment will be reduced drastically or even completely suppressed within PBEsol+U method, and the total density of states reveal that the system with Mg vacancy displays a p-type conductivity character.

I. Introduction

A material that exhibits both ferromagnetic and wide bandgap properties offers the exciting prospect of combining nonvolatile magnetic storage with conventional semiconductor (insulator) electronics in a single device. This material offers a number of interesting possibilities in the pursuit of "spintronics", which is a branch of science and technology that exploits novel electronic devices.[1] In this case, how to promote magnetism in a semiconductor (insulator) is the key to solving the problem. Since Venkatesan and Coey[2] discovered the unexpected ferromagnetism in undoped HfO$_2$ thin film, the so-called "d^0 magnets" brought new opportunities to spintronics, and thus were attracted great attention. Broadly speaking, the

---
[a]Author to whom correspondence should be addressed. Electronic mail: scu_kuangxiaoyu@163.com.

term d^0 magnets referred to a class of materials which, lacking any magnetic ions with open d or f shells, should in principle not be ferromagnetic, but nevertheless exhibited signatures of ferromagnetism often with a Curie temperature exceeding 300 K.[3] Subsequent investigations were mainly focused on the ferromagnetism of closed-shell oxides doped with nonmagnetic elements[4] or undoped oxides[5]. Shortly after, there were similar reports of ferromagnetism for other oxides such as TiO_2,[6] ZnO,[7] MgO,[8] etc. Among these, MgO has wide bandgap rocksalt structure without d or f shells, and thereby it is one of the most attractive model materials for investigating d^0 ferromagnetism. Notably, MgO is also certainly the most important barrier material for magnetic tunnel junctions.[9] Thus, characterization of magnetism of MgO is an interesting issue, which is essential to further study on "d^0 magnets".

Magnetism induced by intrinsic defects in MgO were attracted much attention in the last few years. Experimentally, Hu *et al.* demonstrated that neutral Mg vacancies at the surface of nanograins were responsible for the room temperature in MgO nanocrystalline powders prepared by sol-gel method.[8] By applying the element specificity of the x-ray magnetic circular dichroism technique on the MgO thin film, Martínez-Boubeta *et al.* showed that the magnetic moment arisen from the spin polarization of the 2p electrons of oxygen atoms surrounding Mg vacancies.[10] And Araujo *et al.* further observed robust ferromagnetic ordering well above room temperature in pure transparent MgO thin film, which was deposited by different techniques.[11] Lately, Photoluminescence and x-ray photoelectron spectroscopies also revealed that the ferromagnetism in the MgO thin film was correlated directly with the Mg vacancies.[12] These studies open up researchers' enthusiasms for MgO. However, until now, no group experimentally showed that MgO bulk exhibited ferromagnetism. Thus, the characterization of magnetism of MgO is still unclear. Back in 2007, Stoneham *et al.* pointed out that the cation vacancy in MgO could be experimentally found in two charging states: neutral, V_{Mg}^0, and singly charged, V_{Mg}^-,[13] hence the magnetism induced by intrinsic defects maybe also related to the charged defects. Additionally, Kumar *et al.* reported that oxygen vacancies and adsorption of hydrogen species can contribute to the room temperature ferromagnetism of MgO nanocrystallites,[14] nevertheless most of theory calculations focused on cation vacancies in rocksalt MgO. Hardly any of investigations reported about anion vacancy with different charge states. Thus, further studies which are focused on the characterization of magnetism of cation/anion vacancies in MgO with different charge states are of urgency and necessity. In consistent with experiments, theory calculations also found that cation vacancy can introduce magnetic moment to the defect system, but the ferromagnetism of MgO remains controversial to date. Based on density functional theory (DFT) with

generalized gradient approximation (GGA), Wang *et al*. reported that the magnetic moment in MgO bulk with Mg vacancies was origin from the partially occupied O 2p orbitals,[15] which was similar to the mechanism of CaO[16]. They also pointed out that the ferromagnetic state was not stable in the MgO bulk with two Mg vacancies due to the energy difference between the ferromagnetic and antiferromagnetic states being only 28 meV. By contrast, Uchion and Yoko employed the correlation functional of Lee, Yang, and Parr (B3LYP) to MgO cluster with two Mg vacancies and found that the defect cluster had spin-quintuplet state.[17] Resent, Droghetti *et al*. concluded that magnetism originating from 2p orbitals not only depended on the subtle interplay between covalency and Hund's coupling, but also referred to Jahn-Teller distribution.[18-20] The Jahn-Teller distribution is a consequence of correcting Correlation effects of partially filled 2p shells, captured by "+U" or self-interaction correction schemes. Therefore, a comparative study between without and with Correlation effects is also of necessity.

Electronic structure calculations are a powerful tool to describe magnetic nature, even in complicated clustered or nanostructured configurations. In this work, we confine our attention to the characters of magnetism induced by intrinsic vacancy with various charged states in MgO based on first-principles electronic structure calculations. We also investigate the effects of Jahn-Teller distortion by introduction an on-site Coulomb repulsion and Hund's exchange on O 2p states.

II. Computational details

The structural optimization and electronic structure calculations were performed by employing the Vienna *ab initio* simulation package (VASP)[21] code with the projector augmented plane wave[22] basis functions. The exchange-correlation interaction was treated within the PBEsol functional[23] of (GGA), which is a revised Perdew-Burke-Ernzerhof (PBE) and can be enhancement the ground state properties of densely packed solids. The valence configurations were $3s^2$ and $2s^2 2p^4$ for Mg and O. A $2\times2\times2$ supercell containing 64 atoms of host MgO was used to study various vacancies. An energy cutoff of 500 eV was set for the plane wave basis. A $4\times4\times4$ Monkhorst-Pack k mesh[24] over the Brillouin zone was used for the structural optimization while $9\times9\times9$ k mesh used for the density of states (DOS) calculations. Relaxations are performed with standard conjugate gradients algorithm until the Hellman-Feynman force on each ion was less than 0.001 eV/Å. In addition, precluding the fact that standard GGA-PBEsol may underestimate the Coulomb repulsion and tend to overlocalize the charge density, strong correlation effects of 2p open shells were solved by means of PBEsol+U scheme. The PBEslo+U calculations were performed with an on-site Coulomb energy U = 4.6 eV and Hund's exchange J = 1.2 eV applied on the 2p states of O.[25-27]

To quantitatively probe the energetic of the neutral Mg vacancy (V_{Mg}^0) and O vacancy (V_O^0) as well as the O atom substituted by C atom (C_O^0) formation in the host lattice, the formation energy (E_f) can be defined as

$$E_f = E_{tot}(defect) - E_{tot}(perfect) + \mu_{X\text{-vacancy}} - \mu_{X\text{-doped}}, \qquad (1)$$

where $E_{tot}(defect)$ and $E_{tot}(perfect)$ are the total energies of the supercell with and without defect, $\mu_{X\text{-vacancy}}$ and $\mu_{X\text{-doped}}$ are the chemical potential of the atom of vacancy and dopant. In thermodynamic equilibrium, the Mg and O chemical potentials satisfy the equation

$$\mu_{Mg} + \mu_O = \mu_{MgO.} \qquad (2)$$

Here, μ_{MgO} is the chemical potential of MgO bulk and is equal to the total energy of a two-atom unit of bulk MgO, $E(MgO^{bulk})$. Under extreme O-rich condition, μ_O is subject to an upper bound given by the energy of O in an O_2 molecule, $\mu_O^{max} = 0.5E(O_2)$. Correspondingly, μ_{Mg} is derived from the relation

$$\mu_{Mg}^{min} = \mu_{MgO} - \mu_O^{max}. \qquad (3)$$

Under extreme Mg-rich condition, μ_{Mg} is subject to an upper bound given by the energy of Mg in bulk magnesium, $\mu_{Mg}^{max} = E(Mg^{bulk})$. Correspondingly, the upper limit on the magnesium chemical potential then results in a lower limit on the oxygen chemical potential

$$\mu_O^{min} = \mu_{MgO} - \mu_{Mg}^{max}. \qquad (4)$$

Moreover, the carbon chemical potential (μ_C) is determined by the diamond cubic structure. It should be point out that the formation of a point defect strongly depends on the growth or annealing conditions.

III. Results and Discussion

A. Defect formation energy

The present justification is start with the calculations of a perfect $Mg_{32}O_{32}$ supercell. The calculated bond length between Mg and O ($d_{Mg\text{-}O}$) of 2.1034 Å is in good agreement with available experimental data of 2.1056 Å[28], and the obtained heat of formation ΔH_f ($\Delta H_f = E(MgO^{bulk}) - E(Mg^{bulk}) - 0.5E(O_2)$) of 5.65 eV is in reasonable agreement with the experimental data of 6.25 eV measured at the room temperature[29] and is consistent with the result of 5.71 eV calculated by GGA-PW91 method[30]. These imply the chosen functional is suitable for describing MgO system. Then, one neutral atom vacancy (V_X^0, X = Mg and O) is generated by removing one X atom from $Mg_{32}O_{32}$ cell, which corresponds to the vacancy concentration of 3.125%. One neutral carbon atom doping (C_O^0) is constructed by substituting one C atom for O atom, which corresponds to the doping concentration of 3.125%. The calculated formation energies (E_f) for various defects are shown in Figure 1. under O-rich conditions, we can see that the E_f of V_{Mg}^0 is smaller than the

ones of V_O^0 and C_O^0, indicating V_{Mg}^0 more energetically favorable than others in MgO, which is in agreement with the previous calculations.[15,30] Under Mg-rich conditions, the defect formation energies display another relationship, namely, $E_f(V_O^0) < E_f(C_O^0) < E_f(V_{Mg}^0)$. The calculated defect formation energies suggest that our investigation on cation/anion vacancies is more energetically favorable than C doped in MgO.

B. Magnetism induced by single native vacancy

To understand the origin of the magnetic moment in the undoped MgO, we first calculate the total density of state (DOS) of a perfect cubic rocksalt structure MgO with a $2\times2\times2$ supercell, in which the cations are surrounded by octahedral anions with filled valence p bands. The Mg is in a 2+ state due to the donation of its two electrons to the neighbor O atom, which is in a 2- state. The total density of state (DOS) of the perfect MgO is shown in Figure 2(a). The electronic band structure of MgO is divided into three components, including the lower valence bands composed of O 2s orbitals, the upper valence bands composed of O 2p orbitals and the conduction bands composed of Mg 3s orbitals. The calculated band-gap of 5.0 eV is underestimated by almost 3.0 eV with respect to the corresponding experimental value[28]. The underestimation of the band-gap within DFT theory is a consequence of the single-particle approximation that has been used here. In accordance with other reports in the literatures[15,30], the density of states (DOS) of perfect MgO is identical for both projections of spin. The corresponding integral of the total DOS is shown in Figure 2(b). Our evaluated integrals are 64 states over O 2s orbital level and 256 states over Fermi level, indicating that the O 2s and O 2p orbitals have fully occupied. Furthermore, the total magnetic moment of the perfect system is zero. Based on these points, the magnetic moment impossible exists in the perfect MgO.

Afterwards the influence of vacancies upon the magnetism in the MgO bulk is studied. In MgO, there are two kinds of possible native point vacancies, which are Mg vacancy (V_{Mg}) and O vacancy (V_O). The charge states of the native vacancies in MgO can be 0, ±1, ±2. So there are six kinds of native defects, namely, V_{Mg}^0, V_{Mg}^-, V_{Mg}^{2-}, V_O^0, V_O^+ and V_O^{2+}. We focus on single Mg vacancy in MgO for first. The neutral Mg vacancy V_{Mg}^0 is formed by removing one Mg atom, leading to Mg vacancy concentration of 3.125%. The singly charged Mg vacancy V_{Mg}^- and closed shell Mg vacancy V_{Mg}^{2-} are simulated by adding one and two electrons to the center of the neutral Mg vacancy. After relaxation, all three kinds of charged Mg vacancies do not distort the cubic structure. The relaxed Mg-O distance and total magnetic moments are summarized in Table I. For V_{Mg}^0, the Mg-O distance decreases slightly by 0.0020 Å compared to perfect MgO and brings a local magnetic moment of 1.9260 μ_B. As V_{Mg}^- (V_{Mg}^{2-}) is introduced into the supercell, the oxygen atoms

5

around the vacancy exhibit large outward relaxations of about 4.4% (10.0%) with respect to the equilibrium Mg-O distance (2.1034 Å). It is found that V_{Mg}^- also introduces a local magnetic moment of 0.9418 μ_B, while V_{Mg}^{2-} does not carry any magnetic moment.

To visualize the changes upon the electronic structures, the spin-resolved total DOSs of the MgO bulk with V_{Mg}^0, V_{Mg}^- and V_{Mg}^{2-} are shown in Figure 3. As can be seen from Figure 3(a), spin splitting occurs at all the valence band area and the Fermi level (E_F) penetrates the top of the valence band. It demonstrates that V_{Mg}^0 introduces holes in MgO, which is reasonable because V_{Mg}^0 needs two more electrons from the lattice. In this case, the spin-up states are completely occupied and the spin-down states are partially occupied, leading to formation magnetic moment. For V_{Mg}^-, Figure 3(b) gives rise to the asymmetric occupied levels of spin-up states and spin-down states, and E_F passes through the spin-down states, indicating that V_{Mg}^- also creates magnetic moment. That is because V_{Mg}^- also introduces one hole into MgO. For V_{Mg}^{2-} (see Figure 3(c)), it can be seen that up and down spins are symmetric without polarization, indicating that V_{Mg}^{2-} can not create magnetic moment. Figure 3 also shows that E_F is mainly dominated by O 2p orbitals, which indicates that magnetic moment is mainly induced by O 2p orbitals. So the origin of magnetic moment can be explained as: V_{Mg}^0 and V_{Mg}^- lead to loss of donor charges, and holes formed of O 2p orbitals try to compensate the loss of electrons. The process leads to a redistribution of the electronic bands. To further emphasize the nature of magnetism, an isosurface plot of spin density distribution of V_{Mg}^0 in MgO is shown in Figure 4. It is evident that the spin polarization is strongly localized at the six oxygen atoms surrounding the Mg vacancy, with a small contribution from the further O atoms. Similar moment distributions are found in V_{Mg}^-, which are not shown here. Thus, we conclude that the origin of magnetism by V_{Mg}^0 (or V_{Mg}^-) is largely due to the spin polarization of the surrounding O atoms.

Can similar behavior be noticed for O vacancy in MgO? We take our calculations in a $2\times2\times2$ supercell of MgO with three different charge states, namely, V_O^0, V_O^+ and V_O^{2+}. After full relaxation, the system remains rocksalt structure. Compared with perfect MgO, the Mg-O distance (shown in Table I) slightly relax outward by 0.1%, 1.1%, and 2.2% for V_O^0, V_O^+ and V_O^{2+}, respectively. The total magnetic moment of three charged defects is zero, suggesting that O vacancy in MgO can not induce magnetic moment. The corresponding total spin-resolved DOSs are shown in Figure 5. It can be seen that all of them do not reveal spin polarization and do not change the shape of the total DOSs with only an impurity state in the band structure of MgO. For V_O^0 (Shown in Figure 5(a)), the electronic structure calculation gives a nonmagnetic state, and the orbital levels move to the lower energy level. Further, V_O^0 does not destroy the

insulating behavior but decreases the band gap. Since one V_O^+ induces one more electron and one V_O^{2+} vacancy induces two more electrons, their orbital levels continue to shift lower energy level, and E_F move upward. However, their electron behavior is different from the one of V_O^0. Both Figure 5(b) and 5(c) show that the classical insulator material MgO becomes a conductor because E_F crosses the conduction band, showing an n-type material behavior. That is because that V_O^+ (V_O^{2+}) can introduce one (two) excess electron(s), which can possibly move E_F into conduction band, behaving typical electron donors. In summary, only V_{Mg}^0 and V_{Mg}^- can introduce magnetism into MgO, while V_{Mg}^{2-} and various charged O vacancies can not be, indicating that the magnetism in undoped MgO is mediated by holes and destroyed by electrons.

C. The mechanism of the magnetism

Our first-principles calculations show that single Mg vacancy with neutral or singly charged can induce magnetic moment into MgO host. It can be understood by using a group theory. As mentioned above, Mg cations are surrounded by an octahedron of six O anions in perfect MgO. The symmetry of this octahedron crystal field belongs to O_h. When MgO introduces single Mg vacancy, the O_h symmetry is well preserved regardless of the charged defects. As shown in Table I, only the Mg-O distance changes slightly compared to that of the perfect MgO. From the molecular orbital theory, the linear combination of the σ-type atomic orbitals of the central metal forms σ-type molecular orbitals. According to group theory, the irreducible representations of these σ-type molecular orbitals are split into singlet a_{1g} state, triplet t_{2g} states and doublet e_g states.

The schematic energy level diagram of σ-type molecular orbitals is illustrated in Figure 6. For perfect MgO, the highest energy levels for electrons are doublet e_g states, which are fully occupied. As shown in Figure 6(b), V_{Mg}^0 leads to the partially occupied e_g states. The electronic configuration of V_{Mg}^0 is $a_{1g}^2 t_{1u}^6 e_{g+}^2$, leading to a net of spin S = 1. Thus, V_{Mg}^0 results in a spin-triplet state with a magnetic moment of 2 μ_B. As seen from Figure 6(c) and 6(d), V_{Mg}^- and V_{Mg}^{2-} configurations have one and two more electrons than the one of V_{Mg}^0. In this case, one and none holes are located in e_g states, and corresponding the electronic configuration turns $a_{1g}^2 t_{1u}^6 e_{g+}^2 e_{g-}^1$ and $a_{1g}^2 t_{1u}^6 e_g^4$, leading to a net of spin-doublet with a magnetic moment of 1 μ_B and a net of spin-singlet with a magnetic moment of 0 μ_B, respectively. The slight decrease in the magnetic moment from our first-principles calculations is due to the distortion of lattice.

D. Magnetism induced by double neutral Mg vacancies

Since single neutral Mg vacancy appears to play a more important role on the magnetism of MgO

system, it is further interesting to study the case of double neutral Mg vacancies. We form double neutral Mg vacancies in MgO by removing two Mg atoms from a $2\times2\times2$ supercell of MgO. The corresponding concentration of Mg vacancies is 6.125%. We consider five different configurations of the double neutral Mg vacancies in the supercell, as shown in Figure 7. For convenience, five configurations are labeled as $V_{Mg1}V_{Mg2}$, $V_{Mg1}V_{Mg3}$, $V_{Mg1}V_{Mg4}$, $V_{Mg1}V_{Mg5}$ and $V_{Mg3}V_{Mg5}$, the V_{Mg}-V_{Mg} distance in the perfect supercell corresponds to 2.9746 Å, 4.2068 Å, 5.1522 Å, 5.9493 Å and 7.2863 Å, respectively. After structural relaxation, five different configurations have nearly the same equilibrium volume and decrease slightly compared to perfect supercell as shown in Table II, along with the defect formation energies and magnetic moments. Among these configurations, $V_{Mg1}V_{Mg3}$ has the lowest formation energy, suggesting that two Mg vacancies tend to form at the second nearest sites. $V_{Mg1}V_{Mg5}$ has the highest formation energy, meaning that this configuration is the most unstable. The calculated magnetic moment decreases with the separation distance increasing, indicating that the separation distance between two Mg vacancies certainly affects the magnetic coupling.

To shed more light on the difference of magnetic coupling of these different configurations, we show the spin density distribution around Mg vacancies in Figure 8. It reveals that most of the spin density is localized at the nearest neighboring O atoms around Mg vacancy and with a small contribution from the further O atoms. Shown in Figure 8, we define a coordinate system with x-axis and y-axis pointing toward horizontal and vertical, while z-axis points out of the xy plane. As mentioned above, the most spin density is localized at the six nearest O atoms around the Mg vacancy. The spin density at the six O atoms is divided into xx-shaped, yy-shaped and zz-shaped. For $V_{Mg1}V_{Mg2}$ configuration (shown in Figure 8(a)), two Mg vacancies are along the diagonal of the xy plane, leading to having two types shaped (xx-shaped and yy-shaped) spin density for the two nearest O atoms in the perpendicular bisectors of the diagonal. The larger spin density along x-axis in Figure 8(b), corresponding to $V_{Mg1}V_{Mg3}$ configuration, is because of the superposition by two xx-shaped. For $V_{Mg1}V_{Mg4}$ configuration (shown in Figure 8(c)), the spin density distribution is symmetric for diagonal, which is similar to the spin density of $V_{Mg1}V_{Mg2}$ configuration. However, V_{Mg4} is far from V_{Mg1}, leading to two O atoms in the lower right corner being weaker spin density than the ones of $V_{Mg1}V_{Mg2}$ configuration. Figure 8(d) shows that the spin density is localized at the nearest neighboring O atoms around V_{Mg1} (or V_{Mg5}) and little extends to other O atoms. The max value of spin density can reflect that the magnetic coupling order of these configurations is $V_{Mg1}V_{Mg3} > V_{Mg1}V_{Mg2} > V_{Mg1}V_{Mg5} > V_{Mg1}V_{Mg4}$. Indeed, the spin density in Figure 6 shows that O atoms around the Mg vacancy are

polarized to different degrees, which are depended on their orientation and distances relative to the Mg vacancy site.

The magnetic coupling of these configurations induced by double neutral Mg vacancies can also be understood from the DOSs. The total DOSs of these configurations (shown in Figure 9) show that the E_F passes through the spin down states, indicating the half metallic characteristic of these configurations. As can be seen, the O 2p states overlap significantly near the E_F, suggesting a strong p-p hybridization interaction between them. PBEsol results reflect that O 2p electrons can couple with each other through p-p interaction.

E. The effects of Jahn-Teller distortion

Theoretical results reported so far are strongly method dependent. The magnetism induced by partially filled O 2p orbitals in simple oxides is sensitive to Jahn-Teller distortion[17-19]. However, calculations based on standard DFT fail to describe the correlation effects of partially filled O 2p orbitals, leading to the erroneous over-delocalization of the charge density, and hence their predictions of magnetism might be overly optimistic. Such correlation effects may be achieved approximately by mixing Hartree-Fock with DFT[19,31], or by self-interaction corrections to DFT[17-19,32], or by DFT plus Hubbard U[19,33]. Recent, most calculations show that DFT plus Hubbard U can correctly describe the strong correlation effects of 2p open shell[25-26,34-35]. In order to explore the Jahn-Teller distortion, three configurations within MgO, namely, single neutral Mg vacancy V_{Mg}^0, singly charged Mg vacancy V_{Mg}^-, and double neutral Mg vacancies of $V_{Mg1}V_{Mg4}$, are examined by PBEsol+U method. After full relaxation, three configurations in supercell undergo a significant Jahn-Teller distortion, with a symmetry lowering and relax outward about 1.2112 $\mathring{A}^3$, 2.1088 $\mathring{A}^3$ and 2.8316 $\mathring{A}^3$ in the equilibrium volume compared to PBEsol results, respectively. The calculated magnetic moment of three configurations is listed in Table III. It is found that the magnetic moment is reduced drastically or even completely suppressed. For $V_{Mg1}V_{Mg4}$ configuration, the obtained magnetic moment of 1.0834 μ_B is about five times of V_{Mg}^0 configuration, indicating that the magnetic moment maybe nonlinear increase with concentration of Mg vacancies increasing. Additionally, calculated results also show that the magnetism induced by Mg vacancies is not enough stable in MgO.

To give a comparative study between PBEsol+U and PBEsol functional, the total spin DOSs by PBEsol+U method are shown in Figure 10. It can be clearly seen that E_F is pinned at the top of valence band, indicating a p-type conductivity character. It should be pointed out that our calculations are not

similar to ASIC and HSE results[19], which shown that both V_{Mg}^0 and V_{Mg}^- exhibited a deep acceptor level in the gap. This demonstrates that the ground state strongly depend on the strength of the U parameter. Indeed, our calculations with an on-site Coulomb energy U = 4.6 eV and Hund's exchange J = 1.2 eV applied on O 2p states are in the right of photoemission and Auger experiments[27]. Further, our results are similar as that the case of Al-doped SiC[36], which also cannot induce obvious magnetic moment and shows a p-type conductivity character.

IV. Conclusions

In summary, we employed density functional theory with PBEsol method to investigate the electronic and magnetic properties of undoped MgO. The results show that V_{Mg}^0 and V_{Mg}^- can introduce magnetic moment to MgO bulk, while V_{Mg}^{2-} does not lead to magnetism in MgO. The induced magnetic moment mainly arises from the 2p orbitals of the nearest O atoms surrounding the Mg vacancy. The origin of the magnetic moment is by holes due to the partially occupied e_{g-} orbitals. It is also found that all of three charged O vacancies can not lead to magnetic moment in MgO. The corresponding density of states show that V_O^0 can not destroy the insulating behavior but decreases the band gap of MgO, nevertheless, V_O^+ and V_O^{2+} change the classical insulator material MgO into an n-type conductor. So we conclude that the magnetism in undoped MgO is mediated by holes and destroyed by electrons. For MgO bulk with double neutral Mg vacancies, the calculated defect formation energies suggest that double Mg vacancies tend to form at the second nearest sites and the calculated magnetic moment decreases with the separation distance increasing. The magnetic coupling driven by two Mg vacancies can be attributed to the p-p hybridization interaction. We also considered the effects of Jahn-Teller distortion via a Hubbard U model. Results show that the magnetic moment induced by Mg vacancy is reduced drastically or even completely suppressed. The total density of states of MgO bulk with Mg vacancies show a p-type conductivity character.

Acknowledgment

Reference

(1) Zunger, A.; Lany, S.; Raebiger, H. *Physics* **2010**, 3, 53.

(2) Venkatesan, M.; Fitzgerald, C. B.; Coey, J. M. D. *Nature* **2004**, 430, 630.

(3) Coey, J. M. D. *Solid State Sci.* **2005**, 7, 660.

(4) Elfimov, I.; Rusydi, A.; Csiszar, S.; Hu, Z.; Hsieh, H.; Lin, H. J.; Chen, C.; Liang, R.; Sawatzky, G. *Phys. Rev. Lett.* **2007**, 98, 137202.

(5) Osorio-Guillén, J.; Lany, S.; Barabash, S.; Zunger, A. *Phys. Rev. Lett.* **2006**, 96, 107203.

(6) Peng, H.; Li, J.; Li, S.-S.; Xia, J.-B. *Phys. Rev. B* **2009**, 79, 092411.

(7) Chan, J. A.; Lany, S.; Zunger, A. *Phys. Rev. Lett.* **2009**, 103, 016404.

(8) Hu, J.; Zhang, Z.; Zhao, M.; Qin, H.; Jiang, M. *Appl. Phys. Lett.* **2008**, 93, 192503.

(9) Parkin, S. S. P.; Kaiser, C.; Panchula, A.; Rice, P. M.; Hughes, B.; Samant, M.; Yang, S.-H. *Nat. Mater.* **2004**, 3, 862.

(10) Martínez-Boubeta, C.; Beltrán, J. I.; Balcells, Ll.; Konstantinović, Z.; Valencia, S.; Schmitz, D.; Arbiol, J.; Estrade, S.; Cornil, J.; Martínez, B. *Phys. Rev. B* **2010**, 82, 024405.

(11) Araujo, C. M.; Kapilashrami, M.; Jun, X.; Jayakumar, O. D.; Nagar, S.; Wu, Y.; Århammar, C.; Johansson, B.; Belova, L.; Ahuja, R.; Gehring, G. A.; Rao, K. V. *Appl. Phys. Lett.* **2010**, 96, 232505.

(12) Li, J.; Jiang, Y.; Li, Y.; Yang, D.; Xu, Y.; Yan, M. *Appl. Phys. Lett.* **2013**, 102, 072406.

(13) Stoneham, A. M.; Gavartin, J.; Shluger, A. L.; Kimmel, A. V.; Ramo, D. M.; Rønnow, H. M.; Aeppli, G.; Renner, C. *J. Phys.: Condens. Matter* **2007**, 19, 255208.

(14) Kumar, A.; Kumar, J.; Priya, S. *Appl. Phys. Lett.* **2012**, 100, 192404.

(15) Wang, F.; Pang, Z.; Lin, L.; Fang, S.; Dai, Y.; Han, S. *Phys. Rev. B* **2009**, 80, 144424.

(16) Elfimov, I. S.; Yunoki, S.; Sawatzky, G. A. *Phys. Rev. Lett.* **2002**, 89, 216403.

(17) Uchino, T.; Yoko, T. *Phys. Rev. B* **2012**, 85, 012407.

(18) Droghetti, A.; Pemmaraju, C. D.; Sanvito, S. *Phys. Rev. B* **2008**, 78, 140404(R).

(19) Droghetti, A.; Sanvito, S. *Appl. Phys. Lett.* **2009**, 94, 252505.

(20) Droghetti, A.; Pemmaraju, C. D.; Sanvito, S. *Phys. Rev. B* **2010**, 81, 092403.

(21) Kresse, G.; Furthmuller, J. *Comp. Mater. Sci.* **1996**, 6, 15.

(22) Kresse, G.; Furthmuller, J. *Phy. Rev. B* **1996**, 54, 11169.

(23) Perdew, J.; Ruzsinszky, A.; Csonka, G.; Vydrov, O.; Scuseria, G.; Constantin, L.; Zhou, X.; Burke, K. *Phys. Rev. Lett.* **2008**, 100, 136406.

(24) Monkhorst, H. J.; Pack, J. D. *Phys. Rev. B* **1976**, 13, 5188.

(25) Zhang, Y.-F.; Liu, H.; Wu, J.; Zuo, X. *IEEE T. Magn.* **2011**, 47, 2928.

(26) Slipukhina, I.; Mavropoulos, Ph.; Blügel, S.; Ležaić, M. *Phys. Rev. Lett.* **2011**, 107, 137203.

(27) Chainani, A.; Mathew, M.; Sarma, D. D. *Phys. Rev. B* **1992**, 46, 9976.

(28) Fei, Y. *Am. Mineral.* **1999**, 84, 272.

(29) Cox, J. D.; Wagman, D. D.; Medvedev, V. A. *CODATA Key Values for Thermodynamics*, 1989, Hwmisphere Pubishing Corp., New York.

(30) Sharma, V.; Pilania, G.; Lowther, J. E. *AIP Adv.* **2011**, 1, 032129.

(31) Heyd, J.; Scuseria, G. E.; Ernzerhof, M. *J. Chem. Phys.* **2003**, 118, 8207.

(32) Pemmaraju, C. D.; Archer, T.; Sánchez-Portal, D.; Sanvito, S. *Phys. Rev. B* **2007**, 75, 045101.

(33) Anisimov, V. I.; Aryasetiawan, F.; Lichtenstein, A. I. *J. Phys.: Condens. Matter* **1997**, 9, 767.

(34) Elfimov, I. S.; Rusydi, A.; Csiszar, S. I.; Hu, Z.; Hsieh, H. H.; Lin, H.-J.; Chen, C.T.; Liang, R.; Sawatzky, G. A. *Phys. Rev. Lett.* **2007**, 98, 137202.

(35) Lany, S.; Zunger, A. *Phys. Rev. B* **2008**, 78, 235104.

(36) Yang, M.; Shi, J. *Phys. Lett. A* **2010**, 374, 3230.

TABLES

Table I. The calculated bond length between Mg and O ($d_{\text{Mg-O}}$) and the total magnetic moments within corresponding defects.

	$d_{\text{Mg-O}}$ (Å)	M (μ_B)
V_{Mg}^{0}	2.1014	1.9260
V_{Mg}^{-}	2.1123	0.9418
V_{Mg}^{2-}	2.1240	0.0004
V_{O}^{0}	2.1057	0.0000
V_{O}^{+}	2.1277	0.0000
V_{O}^{2+}	2.1497	0.0000

Table II. Calculated equilibrium volume V_0, total magnetic moments M and defect formations energies under Mg-rich or O-rich conditions per supercell with double Mg vacancies. The index i in $V_{\text{Mg}i}V_{\text{Mg}i}$ indicates the site for Mg vacancy, shown in Figure 7.

|	V_0 (Å^3)	M (μ_B)	Formation energies (eV)	
			Mg rich	O rich
$V_{\text{Mg1}}V_{\text{Mg2}}$	592.3281	3.9230	18.3953	7.0896
$V_{\text{Mg1}}V_{\text{Mg3}}$	591.8249	3.8556	17.4107	6.1050
$V_{\text{Mg1}}V_{\text{Mg4}}$	592.0933	3.8458	18.3445	7.0388
$V_{\text{Mg1}}V_{\text{Mg5}}$	592.0103	3.8353	18.0623	6.7566
$V_{\text{Mg3}}V_{\text{Mg5}}$	592.1928	3.7835	18.4526	7.1468

Table III. A comparative for calculated equilibrium volume V_0 and total magnetic moments M by PBEsol and PBE+U method.

|	PBEsol		PBEsol+U	
	V_0 (Å^3)	M (μ_B)	V_0 (Å^3)	M (μ_B)
V_{Mg}^{0}	593.9086	1.9260	595.1198	0.1959
V_{Mg}^{-}	603.2021	0.9418	605.3109	0.0019
$V_{\text{Mg1}}V_{\text{Mg4}}$	592.0933	3.8458	594.9249	1.0834

FIGURES
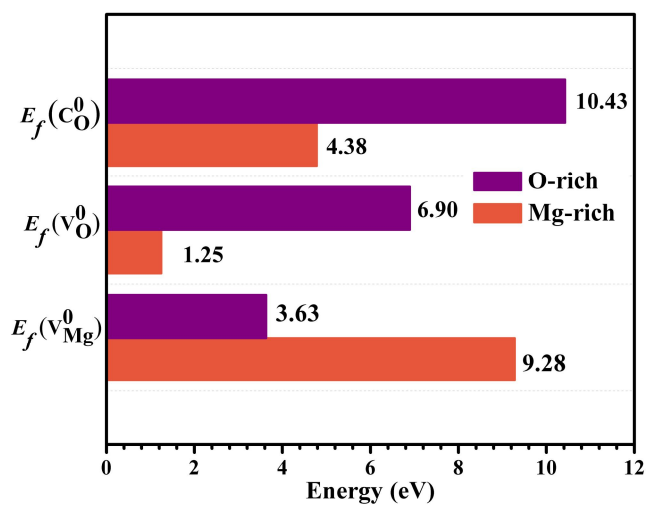
Figure 1 Defect formation energies of a 2×2×2 supercell of MgO. The formation energies are written on the corresponding bars.
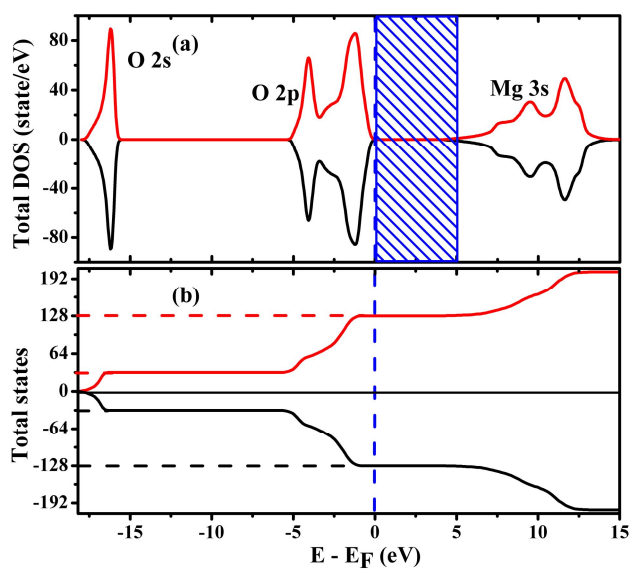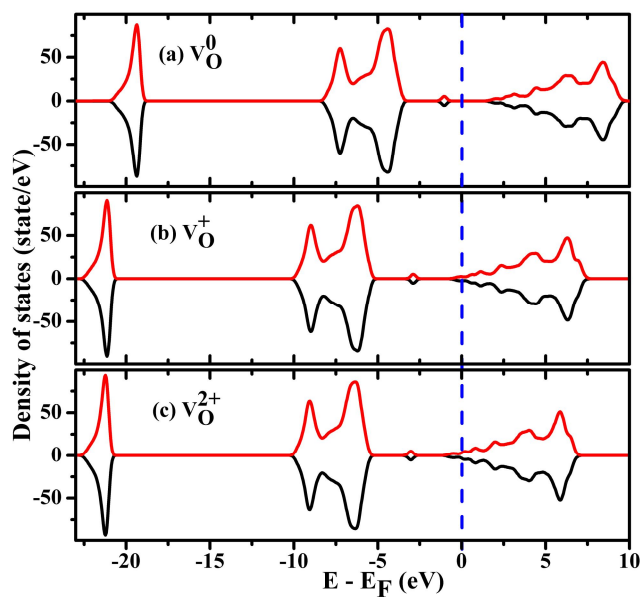

Figure 2 (a) Total density of states for perfect MgO; (b) the corresponding integral of the total density of states.
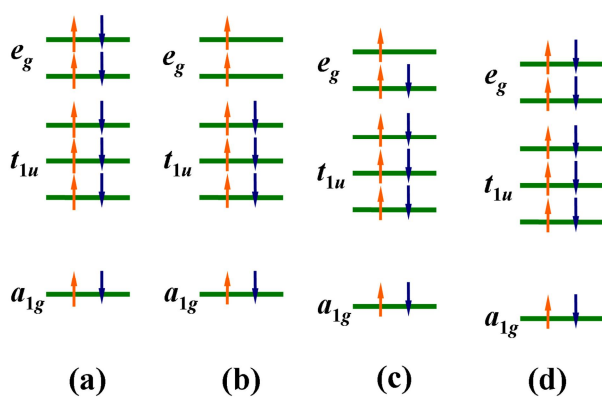
14
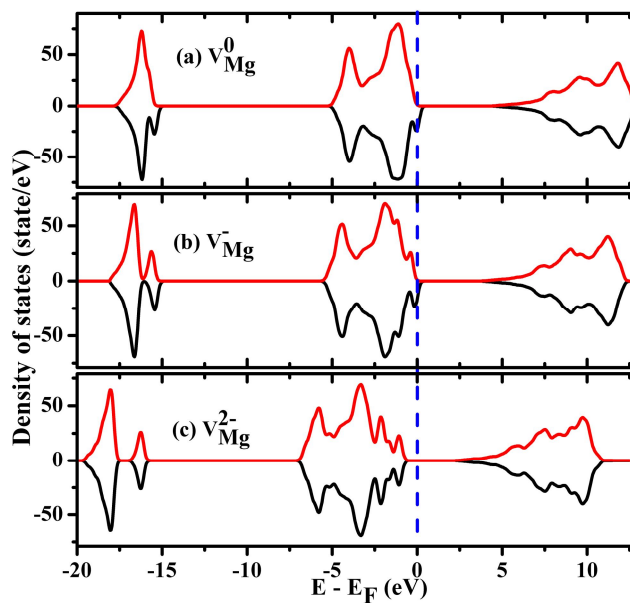
Figure 3 Total density of states of MgO with one (a) neutral V_{Mg}^{0}, (b) single charged V_{Mg}^{-}, and (c) closed shell V_{Mg}^{2-}.
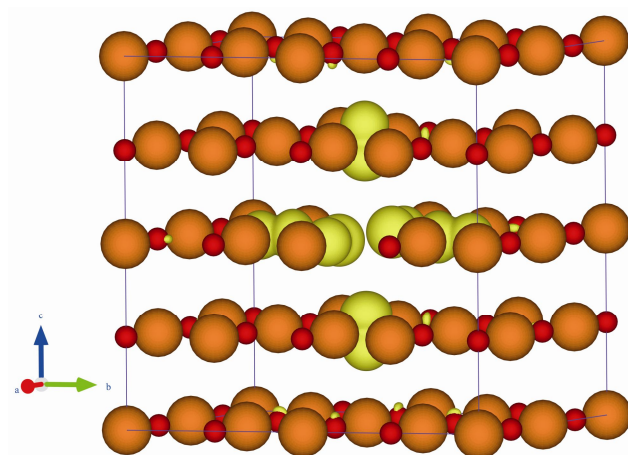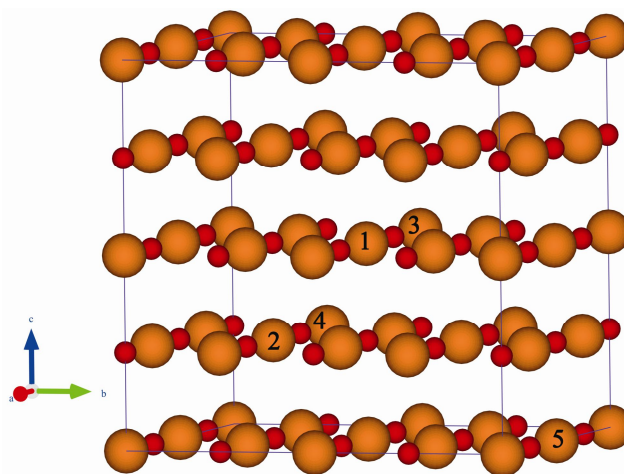

Figure 4 Spin density distribution of a $2\times2\times2$ supercell of MgO with single neutral Mg vacancy. The orange and red balls represent the magnesium and oxygen atoms, respectively.

15
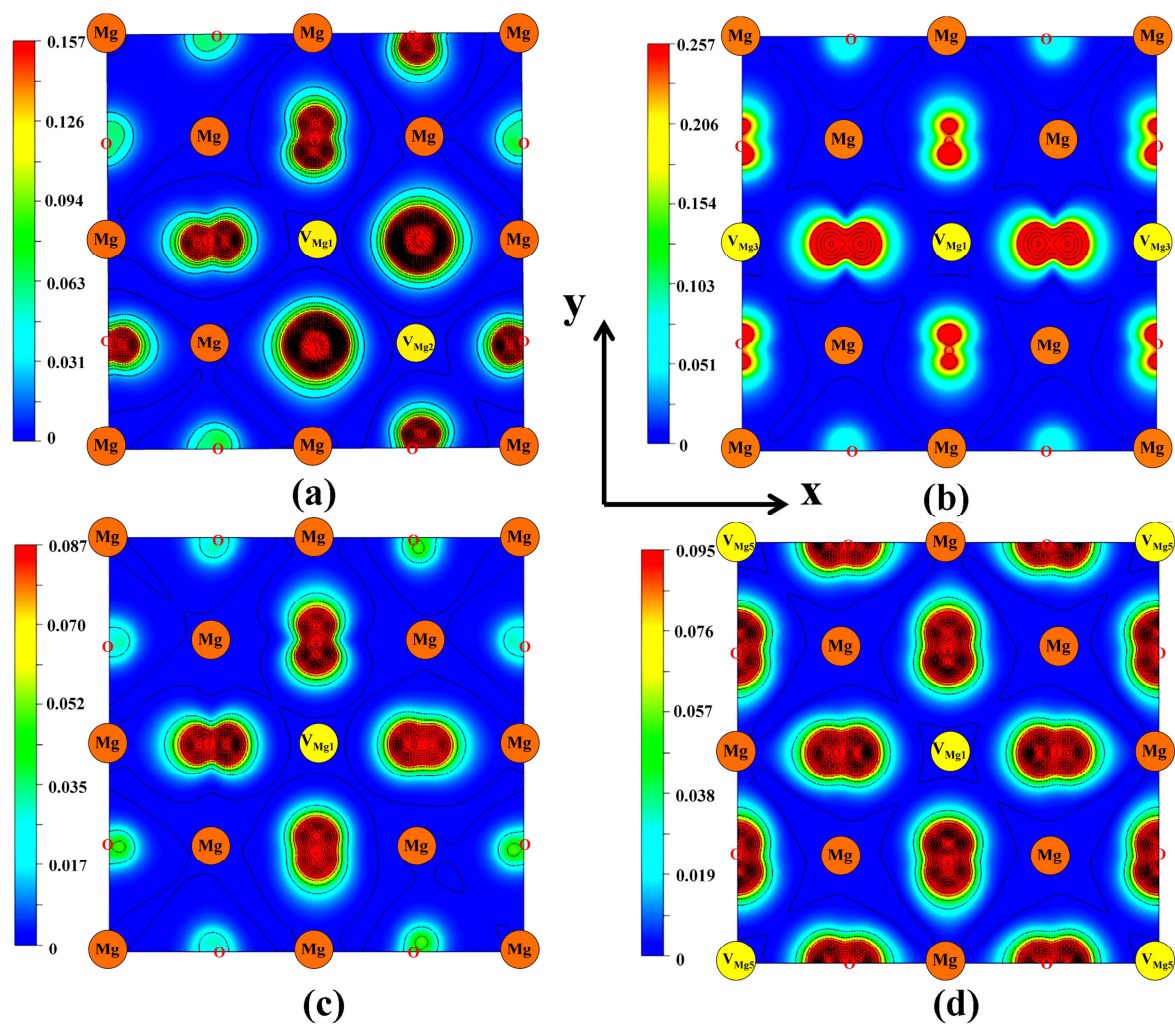
**Figure 5** Total density of states of a MgO supercell containing (a) V_O^0, (b) V_O^+ and (c) V_O^{2+}

**Figure 6** Schematic single particle energy level diagram for (a) perfect MgO, (b) V_{Mg}^0, (c) V_{Mg}^-, and (d) V_{Mg}^{2-}.

Figure 7 A 2×2×2 supercell of MgO. The orange and red balls represent Mg and O atoms, respectively. Numbers 1, 2, 3, 4, 5 denote the positions of Mg vacancies.

Figure 8 Spin density distribution of (a) $V_{Mg1}V_{Mg2}$, (b) $V_{Mg1}V_{Mg3}$, (c) $V_{Mg1}V_{Mg4}$, and (d) $V_{Mg1}V_{Mg5}$ configuration.

17
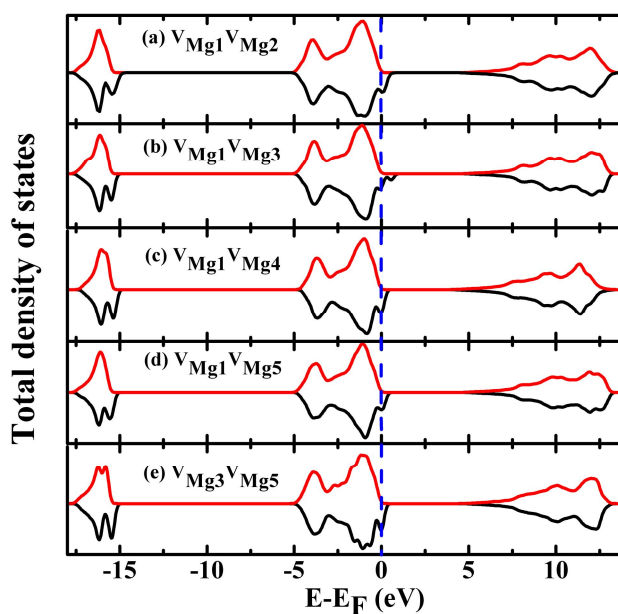
Figure 9 Total density of states for (a) $V_{Mg1}V_{Mg2}$, (b) $V_{Mg1}V_{Mg3}$, (c) $V_{Mg1}V_{Mg4}$, (d) $V_{Mg1}V_{Mg5}$, and (e) $V_{Mg3}V_{Mg5}$ configuration.
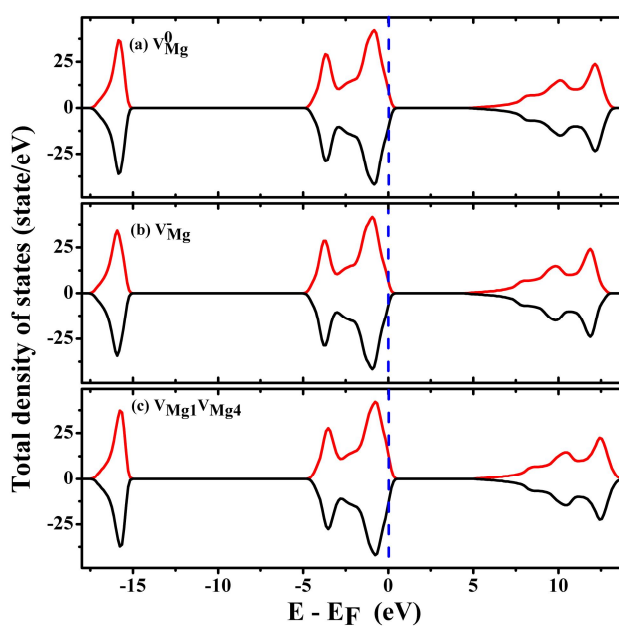
Figure 10 Total density of states for (a) V_{Mg}^0, (b) V_{Mg}^-, and (c) $V_{Mg1}V_{Mg4}$ by PBEsol+U method.